JOURNAL OF SOLID STATE CHEMISTRY 100, 90–100 (1992)

Crystal Chemistry of Anion-Excess ReO_3-Related Phases

II. Crystal Structure of $PrZr_2F_{11}$

J. P. LAVAL* AND A. ABAOUZ

Laboratoire de Céramiques Nouvelles–U.R.A.–C.N.R.S. No. 320, Université de Limoges, 123, Avenue A. Thomas, 87060 Limoges Cedex France

Received October 16, 1991; in revised form February 25, 1992; accepted February 28, 1992

A series of rare-earth fluorozirconates $LnZr_2F_{11}$ (Ln = La, Ce, Pr, Nd) was prepared by solid-state reaction of the binary fluorides and indexed on the basis of single-crystal data. $PrZr_2F_{11}$ crystal structure was determined (R = 0.031) from data recorded on a four-circle automatic diffractometer in the *Ibam* space group, with cell parameters a = 7.716(4) Å, b = 10.006(6) Å, and c = 10.897(6) Å. This structure results from the stacking of alternate single sheets of corner-shared $[ZrF_7]^{3-}$ monocapped trigonal prisms and of $[PrF_8]^{5-}$ square antiprisms. $PrZr_2F_{11}$ structure is closely related to monoclinic β-ZrF_4 type by ordered anionic insertion transforming $[ZrF_7]^{3-}$ monocapped trigonal prisms to $[ZrF_8]^{4-}$ square antiprisms. It also derives from ReO_3 type by a mechanism involving cationic and anionic insertion through a cationic plane net transformation from square 4^4 plane nets to semiregular $3^2.4.3.4.$ ones. Owing to the presence of $LaZr_2F_{11}$ after recrystallization of various fluoride glasses, the description of the cationic subnetwork and of the anionic connections inside this new kind of structure is especially developed in order to give a basis for subsequent investigations of fluoride glass structures.

Introduction

Only few structure types are well characterized in phases involving combinations of rare earth and tetravalent cation fluorides: monoclinic $SmZrF_7$ (*1*), rhombohedral (R-3c) α-MZr_3F_{15} (M = Bi, Y, Ln) (*2, 3*), rhombohedral ($R3m$) β-$PrZr_3F_{15}$ (*4*). Solid solutions based on ReO_3 (*5–7*), tysonite (*8*), $SmZrF_7$ (*5, 6*), and α-$LnZr_3F_{15}$ (*3, 9, 10*) types are also described.

A new Ln fluorozirconate, $LaZr_2F_{11}$, was identified from recrystallization of complex vitreous phases in NaF–BaF_2–AlF_3–LaF_3–ZrF_4 systems (*11*), but its crystal structure was unknown. Owing to the lack of structural information concerning this kind of phase and the structure of fluoride glasses from which it recrystallizes, we carried out, by direct solid-state reaction, the synthesis of $LaZr_2F_{11}$ and of the $LnZr_2F_{11}$ homologous phases. We succeeded in preparing this compound only for the lighter lanthanide cations: La, Ce, Pr, and Nd. Single crystals of good quality were obtained for $PrZr_2F_{11}$ and the crystal structure of this phase was determined.

Experimental

$LnZr_2F_{11}$ phases are easily obtained pure by direct reaction of the binary anhydrous fluorides LnF_3 and ZrF_4 in $\frac{1}{2}$ proportion, heated in a Pt-sealed tube for 1 day at 800°C,

* To whom correspondance should be addressed.

0022-4596/92 $5.00

TABLE I

REFINED CELL PARAMETERS FOR $LnZr_2F_{11}$ COMPOUNDS

Ln	*a* (Å)	*b* (Å)	*c* (Å)	d_{exp}	d_{calc}
La	7.774(4)	10.054(6)	10.999(6)	4.16(6)	4.10
Ce	7.748(4)	10.024(6)	10.959(6)		4.15
Pr	7.716(4)	10.006(6)	10.897(6)	4.25(6)	4.20
Nd	7.687(4)	9.975(6)	10.854(6)		4.27

and then water-quenched. Single crystals of $PrZr_2F_{11}$ are also prepared in Pt-sealed tubes by slow-cooling from 850 to 700°C, annealing for 2 days at 700°C and then water-quenching of a mixture PrF_3–$2ZrF_4$.

$LnZr_2F_{11}$ phases seem strictly stoichiometric under our synthesis conditions and they were indexed in the orthorhombic system, with *Ibam* or *Iba2* space group. Their refined cell parameters are reported in Table I.

A single crystal of light green color and regular quasi-spherical shape was selected for structure investigation. It was considered as a sphere of 0.16 mm diameter and its X-ray pattern recorded on a NONIUS-C.A.D 4 diffractometer with the data collection parameters gathered in Table II. Owing to the low μR coefficient ($\approx$0.6) and the regular shape, no absorption correction was performed.

TABLE II

DATA COLLECTION PARAMETERS

Symmetry: Orthorhombic – space group: *Ibam*
Crystal radius: 0.08 mm
$\mu R = 0.6$
Radiation: Mo $K\alpha$
Scan: $\omega - 2\Theta$
Scan width: $(1. + 0.35\text{tg}\Theta)^\circ$
Aperture: $(3. + 1.\text{tg}\Theta)$ mm
Recording range:
$0 \leq h \leq +12$
$0 \leq k \leq +16$
$0 \leq l \leq +17$
Number of observed reflections: 1061
Number of weak reflections: 309
Number of observed reflections with $I/\sigma(I) > 0.5$: 685
Number of refined variables: 38
No weighting scheme
No absorption correction
$R = 0.031$; $R_w = 0.031$

Structure Determination

The crystal structure of $PrZr_2F_{11}$ was solved in the space group *Ibam* (no. 72) with the program SHELX-76 (*12*), scattering and anomalous dispersion factors for atoms being taken from "International Tables for X-Ray Crystallography" (*13*). Patterson function calculations gave starting coordinates for cations and successive refinements alternating with Fourier difference synthesis allowed us to localize F anions on four sites. The refinement converged to $R = 0.050$ with isotropic thermal coefficients and to $R = 0.031$ after introduction of anisotropic temperature factors, with logical values for all parameters. Neither a weighting scheme nor secondary extinction correction improved the refinement. Attempts to refine the structure in the noncentrosymmetrical *Iba2* space group were also unsuccessful.

The structural refined parameters are reported in Table III and the significant interatomic distances listed in Table IV.

Structure Description

The projection of the $PrZr_2F_{11}$ unit cell content onto the xOy plane is represented in Fig. 1.

A. Anionic Polyhedra

Owing to the presence of only one cationic site for every kind of cation, two different anionic polyhedra can be described and are shown in Fig. 2:

—a $[ZrF_7]^{3-}$ monocapped trigonal prism (M.T.P.). The opposite triangular faces of the trigonal prism are respectively

TABLE III

ATOMIC PARAMETERS AND ANISOTROPIC TEMPERATURE FACTORS ($\times 10^4$) FOR $PrZr_2F_{11}$

At	x	y	z	U_{11}	U_{22}	U_{33}	U_{12}	U_{13}	U_{23}	$B_{eq.}$
Pr	0	0	2500	36(2)	34(2)	55(3)	0	0	0	0.33(2)
Zr	3666.3(11)	1806.9(8)	0	15(3)	23(3)	76(4)	−6(3)	0	0	0.30(3)
F1	5000	0	0	115(35)	27(28)	484(65)	15(35)	0	0	1.65(34
F2	1281(9)	2784(6)	0	85(25)	51(23)	450(48)	29(24)	0	0	1.54(25
F3	2361(7)	765(5)	1294(5)	176(21)	151(19)	287(26)	26(18)	168(21)	68(20)	1.62(17
F4	3992(6)	3148(5)	1360(5)	132(19)	196(21)	318(29)	−30(17)	−6(20)	−174(2)	1.70(18

F_3–F_{33}–F_1 and F_4–F_{41}–F_{22}. The square face F_3–F_{33}–F_{41}–F_4 is capped by F_{21} at the longest distance from Zr: 2.084(4) Å. The average Zr–F bond length ⟨2.042 Å⟩ is slightly shorter than the ones (2.06–2.08 Å) usually encountered for [7]-fold coordinated zirconium (*14*), and the Zr–F distance range is more regular (2.015–2.084 Å) than in $[ZrF_7]^{3-}$ pentagonal bipyramids present in β-$PrZr_3F_{15}$ (1.957–2.167 Å; ⟨Zr–F = 2.076 Å⟩) (*4*).

—an almost regular $[PrF_8]^{5-}$ square antiprism (S.A.). F_3–F_4 distances in both F_3–F_4–F_3–F_4 square sides are quite the same (2.819 and 2.820 Å) and Pr–F bond lengths are very close (Pr–F_3 = 2.373 Å and Pr–F_4 = 2.363 Å). The average ⟨Pr–F⟩ value (2.368 Å) is only slightly shorter than in the $[PrF_9]^{6-}$ tricapped trigonal prism described in the β-$PrZr_3F_{15}$ structure (⟨Pr–F = 2.37(Å⟩) (*4*).

B. Structure Organization

a. Main characteristics. The structure o $PrZr_2F_{11}$ results from the stacking, perpendicular to the Oz axis, of alternate singl

TABLE IV

MAIN INTERATOMIC DISTANCES IN $PrZr_2F_{11}$

M–*M* (Fig. 6)	Zr–F (Fig. 2)	Pr–F (Fig. 2)	F–F (Fig. 2)
Pr–Zr = 4.3230(5)	$-F_1$ = 2.080(6)	$-F_3$ = 2.373(5)	inside M.T.P.:
4.3236(5)	$-F_{21}$ = 2.084(4)	$-F_4$ = 2.363(5)	
Zr–Zr = 4.100(1)	$-F_{22}$ = 2.059(4)		F_{33}–F_3 = 2.820(11)
4.161(1)	$-F_3$ = 2.022(5)		F_{33}–F_1 = 2.592(5) = F_1–F_3
5.317(1)	$-F_4$ = 2.015(5)		F_{33}–F_{41} = 2.697(7) = F_3–F_4
			F_1–F_{22} = 2.428(4)
			F_{33}–F_{21} = 2.601(7) = F_3–F_{21}
			F_{41}–F_{21} = 2.589(7)
			F_{41}–F_{22} = 2.487(7) = F_4–F_{22}
	⟨Zr–F = 2.042⟩	⟨Pr–F = 2.368⟩	F_4–F_{41} = 2.964(10)
			inside S.A.:
			F_{31}–F_{41} = 2.819(7)
			F_{34}–F_{41} = 2.968(7)
			F_{41}–F_{32} = 2.820(7)
			F_{41}–F_{42} = 2.931(10)
			F_{32}–F_{34} = 3.042 (11)

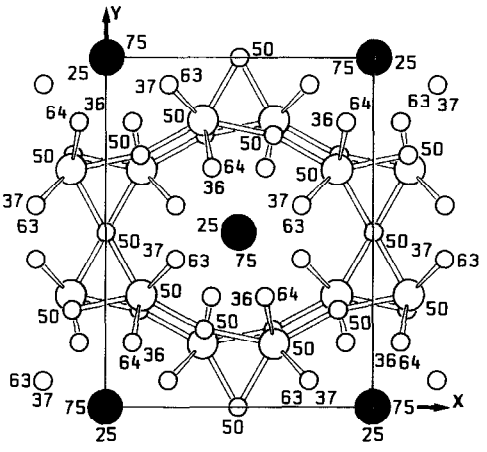

FIG. 1. Projection of $PrZr_2F_{11}$ structure onto xOy plane. Pr = dark large spheres; Zr = light large spheres; F = light small spheres. Numbers indicate z coordinate of atoms ($\times 100$) between 25 and 75. Only Zr–F chemical bonds are drawn.

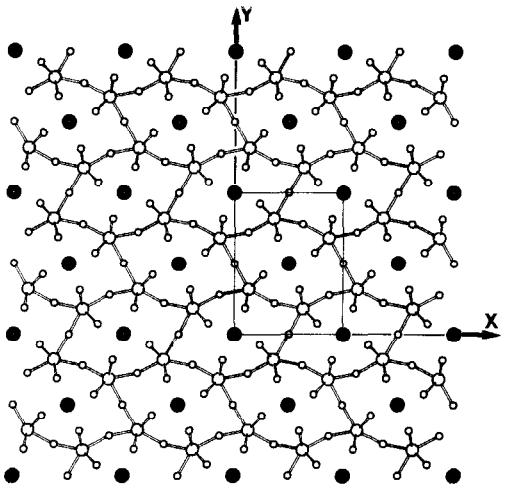

FIG. 3. The (001) projection of a layer (z = 0.50) of corner-shared $[ZrF_7]^{3-}$ monocapped trigonal prisms between two adjacent (twice less dense) Pr layers (z = 0.25 and 0.75). Symbols are the same as in Fig. 1.

sheets of corner-shared $[ZrF_7]^{3-}$ M.T.P. and of $[PrF_8]^{5-}$ S.A. Figures 3 and 4 represent projections of the structure respectively onto the xOy and xOz planes emphasizing layer stacking: Pr layers are twice less dense than Zr ones in accordance with cationic stoichiometry Pr/Zr = $\frac{1}{2}$. Two successive $[ZrF_{5.5}]_n$ sheets are interconnected through F_3 or F_4 vertices of $[PrF_8]^{5-}$ S.A. As both square sides of each S.A. are parallel to zirconium planes and rotated from 45° one by comparison to the other, these two successive $[ZrF_{5.5}]_n$ sheets are also rotated but

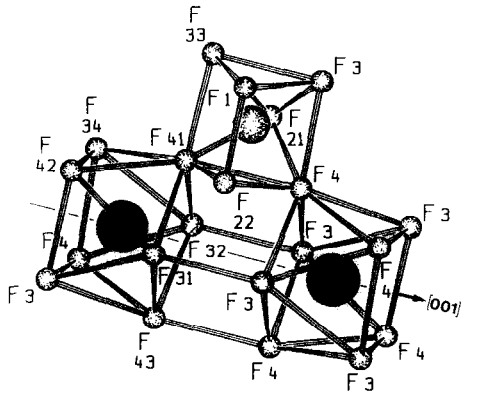

FIG. 2. Perspective drawing of corner-shared $[ZrF_7]^{3-}$ monocapped trigonal prisms and $[PrF_8]^{5-}$ square antiprisms. Along the [001] axis, successive $[PrF_8]^{5-}$ square antiprisms, connected through empty tetracapped cubes, form linear columns.

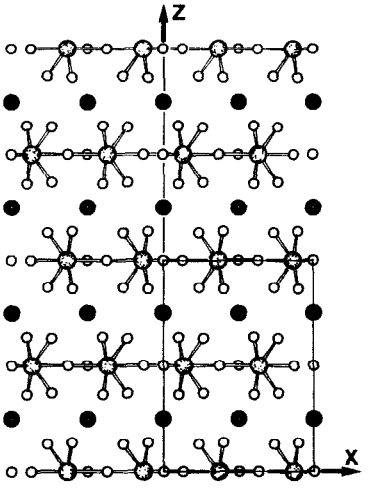

FIG. 4. (010) projection of $PrZr_2F_{11}$ structure, emphasizing layer stacking along the Oz axis. Symbols are the same as in Fig. 1.

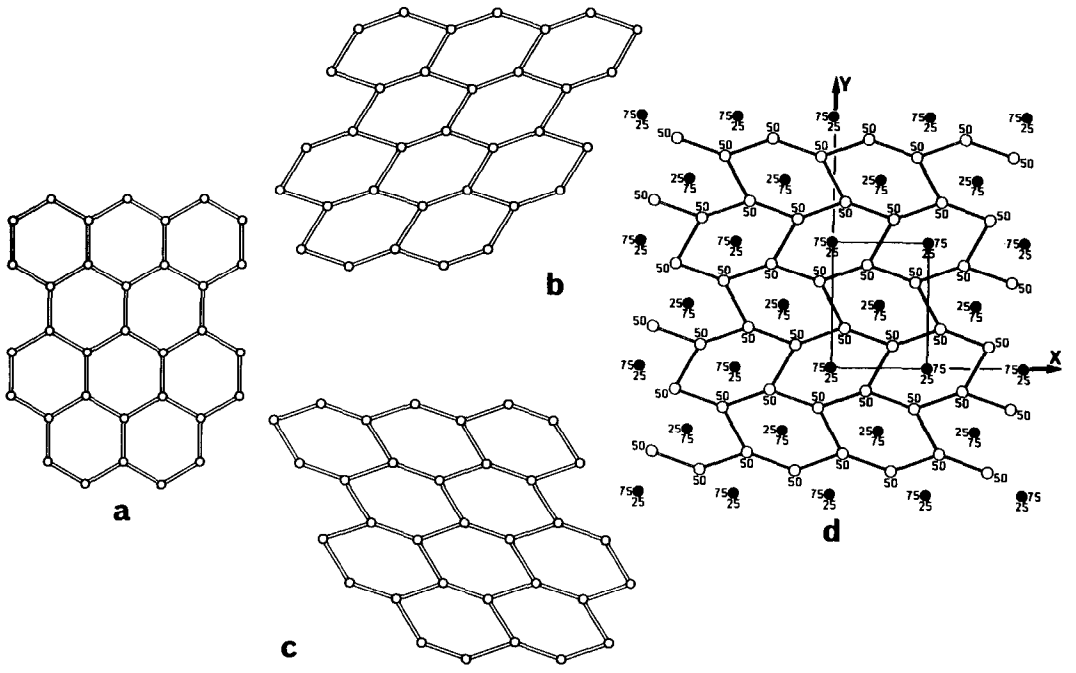

FIG. 5. Transformation of an ideal hexagonal 6^3 plane net (a) to the cationic Zr one of $PrZr_2F_{11}$ (d) through distortion of hexagons (*b/a* of the orthorhombic associated cell decreasing from 1.732 to 1.30). (b) and (c) show both equivalent orientations of the net resulting from the distortion of the hexagonal unit cell. The Zr plane net of $PrZr_2F_{11}$ (d) is formed by a "chemical twinning" process from rows of hexagons parallel to the [100] axis and presenting successively the one and the other orientation along the [010] axis.

only from ≈40°, as clearly evident in Fig. 1. On the contrary, Pr cations are perfectly lined up along the *Oz* axis, forming columns of S.A. separated by empty tetracapped cubes, as partially represented in Fig. 2.

b. Zr plane nets. Plane nets formed by Zr cations in $PrZr_2F_{11}$ can be schematized in two different ways, respectively represented in Figs 5 and 6:

—Considering only Zr cations connected through F corners (Zr–Zr = 4.100 and 4.161 Å), the resulting Zr net (Fig. 5d) is a 6^3 plane one (Fig. 5a), composed of hexagons distorted by moving closer two opposite edges to such an extent that *b/a* (orthorhombic associated cell) becomes ≈1.30 instead of 1.732. In the *a* plane, these flattened hexagons can be orientated in two equivalent directions, as shown on Figs. 5b and 5c. The true Zr plane net corresponds to an intergrowth of parallel single rows of such hexagons lined up along the *Ox* axis and presenting successively, along the *Oy* axis, one and the other orientation, through a "chemical twinning" process on the finest possible scale. It can indeed be imagined other structures containing more complex intergrowths. Such plane net relationships are described by O'Keeffe and Hyde (*14*) for the Zn major net in $BaZn_5$ and $SrZn_5$ alloys.

—Considering also, as on Fig. 6, a Zr–Zr distance of 5.317 Å as significant of some cationic interactions although no direct F connection exists, the Zr plane net in $PrZr_2F_{11}$ is clearly related to a $3^2.4.3.4.$ one

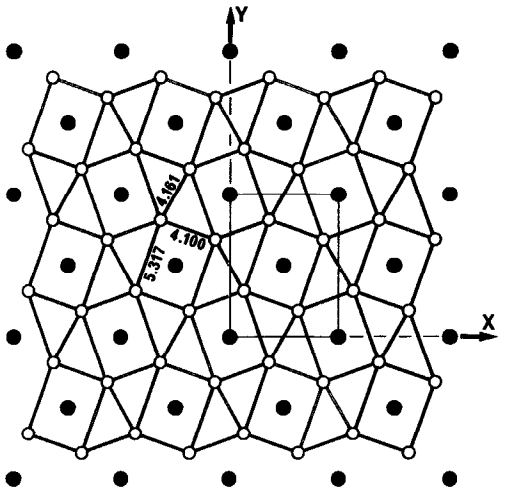

FIG. 6. The (001) projection of Zr plane net with representation of all Zr–Zr distances up to 5.317 Å, emphasizing its structural analogy with a $3^2.4.3.4$. semiregular plane net associating triangular and square groups of atoms (see Al net on Fig. 7).

(Fig. 7), by a lengthening of some Zr–Zr distances (→ 5.317 Å) transforming square groups of cations in rectangular ones. The ideal $3^2.4.3.4$ plane net, thoroughly described by O'Keeffe and Hyde (*14*) is an important semiregular net, intermediate between regular 3^6 (triangular) and 4^4 (square) ones. It derives from a 4^4 square net by a transformation of half square faces into 60° rhombuses (*14, 4*). Similarly elongated $3^2.4.3.4$ nets are present, e.g., in the $NiAl_3$ structure (*15*).

Therefore, the Zr plane net is intermediate between a 6^3 regular hexagonal net ($b/a = 1.732$) and a semiregular $3^2.4.3.4$ one ($b/a = 1.$).

c. 3d-cationic array. The $PrZr_2$ cationic 3d-network of $PrZr_2F_{11}$ presents a close similarity with that of $CuAl_2$ alloy, represented in Fig. 7. This last structure can be described (*15, 16*) as a stacking of regular $3^2.4.3.4$. Al single plane nets alternating with 4^4 single square Cu layers, twice less dense. Each Cu atom is coordinated by eight Al forming a square antiprism. Therefore, as above described for the Zr plane net, the $PrZr_2$ cationic network derives from $CuAl_2$ one by lengthening of some Zr–Zr and Pr–Pr distances along the [010] axis, transforming square groups of cations respectively to rectangular groups in Zr layers and to rhombuses in Pr ones. In spite of this distortion, the layer stacking has the same topology in both structures.

d. 3d-$PrZr_2F_{11}$ structure. The similarity above evidenced between $PrZr_2$ and $CuAl_2$ networks makes easier the description of the complete structure of $PrZr_2F_{11}$ and of the structural relationships with other structure types. Indeed, Zr and Pr polyhedra are exclusively corner-shared through roughly linear Zr–F–Zr and Zr–F–Pr connections and thus, $PrZr_2F_{11}$ could be considered, in first approximation, as an expanded "$CuAl_2$" structure with each anion inserted between two close cations. In fact, this anionic "stuffing" (in the meaning of O'Keeffe and Hyde considering some oxides as "stuffed" alloys (*17*)) affects only three "Zr–Zr" and four "Zr–Pr" connections about each Zr

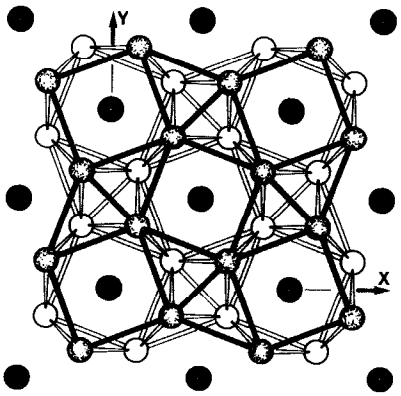

FIG. 7. $CuAl_2$ structure, projected onto the (001) plane, mainly characterized by a stacking of $3^2.4.3.4$. Al single layers alternating along the [001] axis with twice less dense square Cu ones. The upper Al layer is drawn slightly darker. Al = lighter spheres; Cu = dark spheres.

atom of an ideal $CuAl_2$-type $PrZr_2$ network. This regular anionic insertion necessits an adjusting of the Zr cationic net, in order to avoid steric problems, mainly by lengthening of the unbridged Zr–Zr connections inside Zr plane nets (4.100–4.161 → 5.317 Å) and between successive sheets which become completely disconnected. Therefore, although rather formal, such a mechanism of anionic insertion clarifies the main characteristics of the structural organization of $PrZr_2F_{11}$ and confirms the close relationship of its cationic network with the $CuAl_2$ structure.

Comparison with Other Structure Types

A. Comparison with β-ZrF_4 Structure

The structure of β-ZrF_4 (and also of HfF_4, UF_4, and ThF_4, . . . (*18, 19*)) is generally described as a 3-dimensional network of corner-shared $[ZrF_8]^{4-}$ square antiprisms. However, Papiernik *et al.* (*20*) showed that this structure could be considered as a stacking, along the $\underline{Oz}$ axis, of corner-shared $[ZrF_8]^{4-}$ polyhedra forming slightly puckered layers. A structural relationship with the high temperature variety: α-ZrF_4 could then be described. In order to compare β-ZrF_4 and $PrZr_2F_{11}$ structures, it is necessary to consider also in β-ZrF_4 a stacking, along the $\underline{Ox}$ axis, of alternate layers of $[Zr(2)F_8]^{4-}$ and $[Zr(1)F_8]^{4-}$ S.A. In Fig. 8a is represented a projection of the β-ZrF_4 structure onto the yOz plane, emphasizing $Zr(2)F_8$ S.A. connections by removing Zr(1)–F bonds. The comparison with the structure of $PrZr_2F_{11}$ (Figs. 3 and 5d) clearly reveals that both types are closely related. The cationic network is quite the same and most part of anion sites are near identical. Two main differences are to be noted:

—The structure of $PrZr_2F_{11}$ is more symmetrical than that of β-ZrF_4, as attested by the comparison of the unit cell parameters reported in Table V. Successive layers are not exactly superposed, in accordance with $\beta = 94.28°$ of the *I2/c* (nonstandard) monoclinic space group of β-ZrF_4, homologous to the *Ibam* space group of $PrZr_2F_{11}$.

—In β-ZrF_4, successive Zr(2) layers are directly interconnected by F(2) anions, in agreement with the 3-dimensional character of the structure. F(2) anions can be considered as "excess" ones (represented as dark small spheres on Figs. 8a and b), and both structural formula can be written $Pr_4Zr_8F_{44}$ and $Zr(1)_4Zr(2)_8F_{44}F(2)_4$ to underline their similarity.

$PrZr_2F_{11}$ can thus be described as an "ordered anion-deficient β-ZrF_4 phase," all $[Zr(2)F_8]^{4-}$ S.A. being transformed into $[ZrF_7]^{3-}$ M.T.P. (Fig. 8b, to be compared to Fig. 2), without important modifications of the structure.

B. Structural Relationship with ReO_3 Type

In a previous work concerning the structure determination of β-$PrZr_3F_{15}$ (*4*), we described how an ordered F-bridging, between Pr and Zr cations situated in the opposite corners of a quarter of the sides of an ReO_3-type structure, distorted these cationic 4^4 square nets in $[3.4]^3\,[3^2.4^3]^2$ semiregular nets composed of an ordered distribution of square and triangular faces. The structure of β-$PrZr_3F_{15}$ resulting from the stacking of such plane nets was then considered as an "anion-excess ReO_3" phase.

In the same way, if half of the square faces of a 4^4 plane net instead of a quarter are affected by F-bridging, a $3^2.4.3.4.$ plane net is created. As discussed above, the $PrZr_2$ cationic network in $PrZr_2F_{11}$ corresponds to a distortion of $CuAl_2$ type, stacking of $3^2.4.3.4.$ Al layers alternating with 4^4 Cu ones. Moreover, the $CuAl_2$ structure derives from $PtHg_2$ type (cationic subcell of Fig. 9a) by a $4^4 \rightarrow 3^2.4.3.4.$ topological transformation (*14, 16*). $PtHg_2$ itself is a deficient bcc array with one-fourth of its cations missing and a ccp Hg packing. A structural relationship between ReO_3 and $PrZr_2F_{11}$ (and

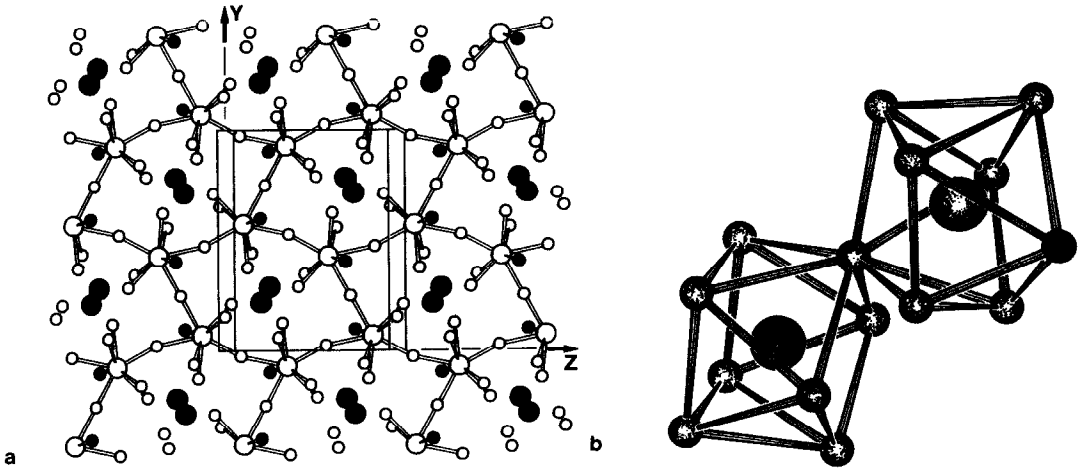

FIG. 8. (a) Projection of β-ZrF_4 structure onto the yOz plane. Zr(1)–F bonds are removed in order to emphasize the similarity with $PrZr_2F_{11}$ structure. (b) Perspective drawing of $[ZrF_8]^{4-}$ polyhedra in β-ZrF_4 structure, represented with the same orientation as homologous polyhedra in $PrZr_2F_{11}$ (Fig. 2). "Excess anions" F_2 are represented as dark small spheres. Zr(1) atoms, homologous to Pr ones in $PrZr_2F_{11}$, are drawn as dark large spheres. Zr(2) atoms, homologous to Zr ones, are light large spheres.

also β-ZrF_4), less direct however than between ReO_3 and β-$PrZr_3F_{15}$, can then be proposed. It involves several steps, represented in Fig. 9, through well known structural processes:

1. Ordered cationic insertion in half cuboctahedral holes of ReO_3 structure gives an $A_{0.5}BX_3$ (or AB_2X_6) structure, intermediate between ReO_3 and perovskite types, with a $PtHg_2$-type cationic subcell (Fig. 9a).

2. Disconnection along the Oz axis of corner-shared BX_6 octahedra and A cations in alternate layers, transforming the AB_2X_6 structure to an AB_2X_8 one, similar to $TlAlF_4$ type (*21*) with half Tl cations missing (Fig. 9b).

3. Anionic bridging through half square faces of octahedra layers, with shortening of the B–B concerned distances transforms the 4^4 B square nets to $3^2.4.3.4.$ ones, without modifications of the A layers (Fig. 9c). The formula becomes AB_2X_9.

4. After breaking of half B–X–B connections (all the ones orientated along the $Oy(PrZr_2F_{11})$ direction) of the square faces of the $3^2.4.3.4.$ plane nets, an insertion of excess anions associated to axial ones changes each B–X–B broken connection into 2 B–X bonds. This operation generates anionic square antiprisms about A cations (Fig. 9d). At last occurs a reorganization of the structure involving lengthening of B–B disconnected distances in order to avoid steric constraints as previously discussed. After this step, the formula reaches its final value: AB_2X_{11}.

TABLE V

COMPARISON OF $PrZr_2F_{11}$ AND β-ZrF_4 UNIT CELLS

$PrZr_2F_{11}$		β-ZrF_4	
a (Å)	7.716	c (Å)	7.73
b (Å)	10.006	b (Å)	9.57
c (Å)	10.897	a (Å)	9.93
β (°)	90.0	β (°)	94.28
Space group	*Ibam*		*I2/c*

For β-ZrF_4, the transformation steps are almost the same but, owing to the 3-dimen-

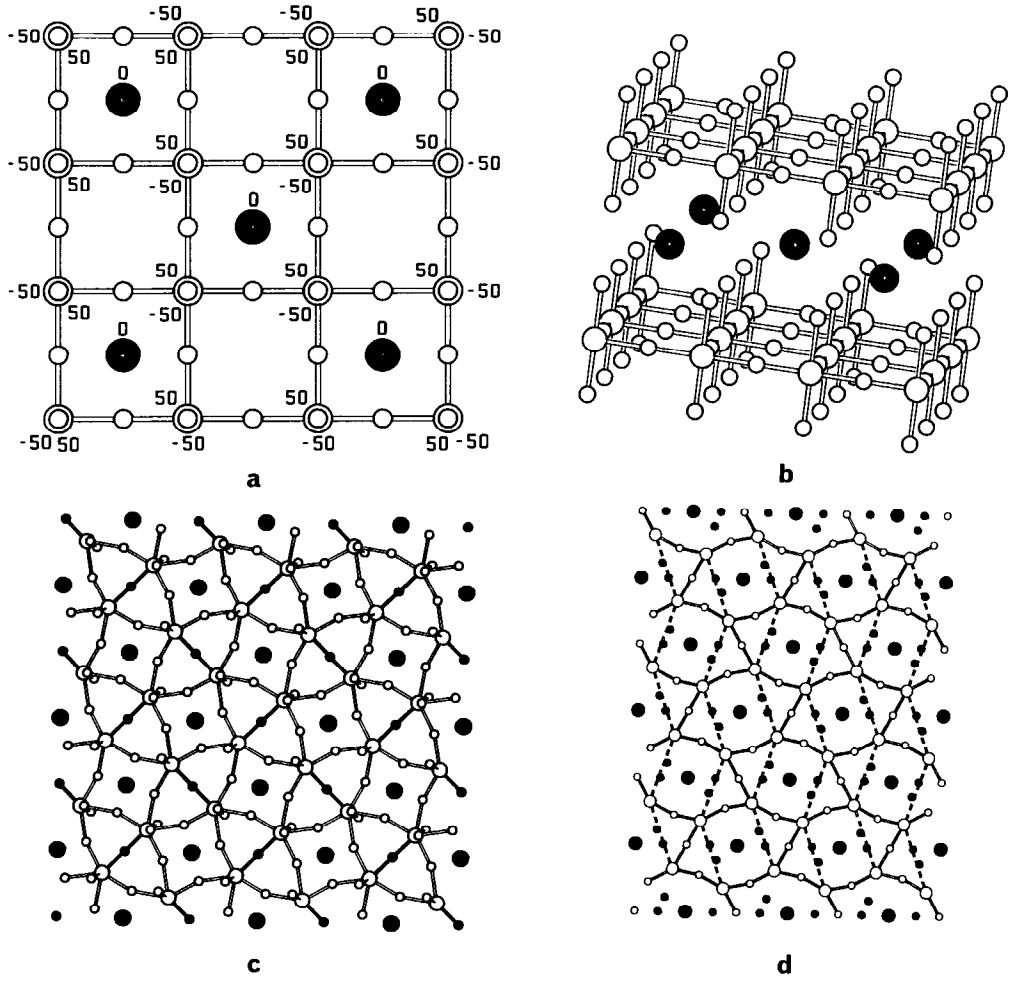

FIG. 9. Structural relationship between $PrZr_2F_{11}$ and ReO_3: (a) Step 1: $A_{0.5}BX_3(AB_2X_6)$ structure derived from ReO_3 type by ordered cationic insertion in half cuboctahedral holes ("$PtHg_2$" cationic network). (b) Step 2: AB_2X_8 ("$Tl_{0.5}AlF_4$") structure resulting from pulling apart BX_6 layers. (c) Step 3: AB_2X_9 structure, after ordered anionic bridging (dark small spheres and bonds) between B cations, transforming the 4^4 B square net to a $3^2.4.3.4.$ one ($PtHg_2 \rightarrow CuAl_2$ cationic network). (d) Step 4: AB_2X_{11} structure derived from AB_2X_9 one by breaking half Zr–F–Zr connections (dotted lines) and inserting excess anions (dark small spheres). Lengthening of broken Zr–Zr connections and anionic local reorganization lead to the real structure of Figs. 3 and 5d. A cations = dark large spheres; B cations = light large spheres; X anions = light small spheres.

sional character of this structure, the disconnection of step 2 affects only half axial anions, alternately above and under the octahedra plane net, in rows parallel to the $Oz(\beta\text{-}ZrF_4)$ axis (Fig. 8a). That leads to a formula AB_2X_7 which, after step 3, becomes AB_2X_8. Since one F anion for each Zr atom stays bound between two consecutive Zr(2) layers, two excess anions are to be inserted for each Zr(2) cation in step 4 in order to obtain the final formula AB_2X_{12}.

One could object to the above structural

relationship between $PrZr_2F_{11}$, β-ZrF_4, and ReO_3 because of a rather high complexity which could raise questions about its real meaning. In fact, this complexity results from the conjunction of two structural transformations:

—a classical change from a three-dimensional ReO_3 structure to a layer one, composed of alternate sheets of octahedra and of high size cations (steps 1 and 2),

—an introduction of anion excess inside this layer structure by two different ways: an anionic bridging by the same mechanism as described for β-$PrZr_3F_{15}$ (*4*) and α-YZr_3F_{15} (*3*) (step 3) and then a new anionic insertion through breaking of some Zr–F–Zr connections (step 4).

Therefore, the simplest way to link $PrZr_2F_{11}$, β-ZrF_4 (and other analogous phases) to ReO_3 type is to consider that the previous mechanisms of anionic insertion can be applied as well directly to ReO_3 type, like in β-$PrZr_3F_{15}$ (*4*) and α-YZr_3F_{15} (*3*), as to various structure types deriving from ReO_3. That foreshadows a forthcoming comparison (*22*) of various fluoride structures, mainly differing from one another by similar changes in anionic connections.

Conclusion

The structure of $PrZr_2F_{11}$ is a new original framework of corner-shared $[ZrF_7]^{3-}$ M.T.P. and $[PrF_8]^{5-}$ S.A. associated in alternate layers, and perfectly homologous to β-ZrF_4 (corner-shared $[ZrF_8]^{4-}$ S.A.) by ordered formation of anionic vacancies.

In the present study, the description of the cationic network is especially emphasized and displays a great usefulness to understand the main features of $PrZr_2F_{11}$, considering the extensive already published work concerning, e.g., plane net relationships and topological transformations in basic structure types.

After $SmZrF_7$, α- and β-$LnZr_3F_{15}$, $PrZr_2F_{11}$ is the fourth original structure type described in LnF_3–MF_4 systems. All these phases present a common characteristic: they are structurally related, more or less directly, to ReO_3 type by classical geometrical transformations, mainly crystallographic shear ($SmZrF_7$), and anion insertion and bridging inside empty square faces (α- and β-$LnZr_3F_{15}$). For $PrZr_2F_{11}$ and β-ZrF_4, the relationship with ReO_3 type is not direct and it is easier to consider that these phases derive by anion excess from an intermediate layer structure composed of alternate sheets of octahedra and of isolated cations like that represented in Fig. 9b.

It is very likely that, like $PrZr_2F_{11}$ and β-ZrF_4, numerous fluoride phases of zirconium will be structurally related by anion excess to ReO_3 or to derived structure types, like perovskite, bronzes, ... This will be the subject of forthcoming papers.

Acknowledgement

The authors are grateful to Professor D. Avignant (Clermont-Ferrand University) for X-ray data collection.

References

1. M. Poulain, M. Poulain, and J. Lucas, *J. Solid State Chem.* **8,** 132 (1973).
2. E. Caignol, J. Metin, R. Chevalier, J. C. Cousseins, and D. Avignant, *Eur. J. Solid State Inorg. Chem.* **25,** 399 (1988).
3. J. P. Laval and A. Abaouz, in preparation.
4. J. P. Laval and A. Abaouz, *J. Solid State Chem.* **96,** 324 (1992).
5. M. Poulain, M. Poulain, and J. Lucas, *Mater. Res. Bull.* **7,** 319 (1972).
6. M. Poulain, M. Poulain, and J. Lucas, *Rev. Chim. Miner.* **12,** 9 (1975).
7. J. C. Champarnaud-Mesjard, J. P. Laval, and B. Gaudreau, *Rev. Chim. Miner.* **11,** 735 (1974).
8. R. E. Thoma, H. Insley, and G. D. Brunton, *J. Inorg. Nucl. Chem.* **36,** 1095 (1974).
9. Yu. M. Korenev, P. I. Antipov, and N. V. Novoselova, *Zh. Neorg. Khim.* **25,** 1255 (1980).
10. G. Fonteneau and J. Lucas, *J. Inorg. Nucl. Chem.* **36,** 1515 (1974).
11. J. M. Parker, A. B. Seddon, and A. G. Clare, *Phys. Chem. Glasses* **28**(1), 4 (1987).

12. G. M. SHELDRICK, "SHELX76, Program for Crystal Structure Determination," Cambridge University, Cambridge (1976).
13. "International Tables for X-ray Crystallography," Kynoch Press, Birmingham (1968).
14. M. O'KEEFFE AND B. G. HYDE, *Philos. Trans. R. Soc. London, Ser. A* **295,** 553 (1980).
15. K. SCHUBERT, "Kristallstrukturen Zweikomponentiger Phasen," Springer-Verlag, Berlin (1964).
16. B. G. HYDE AND S. ANDERSSON, "Inorganic Crystal Structures," Wiley, New York (1989).
17. M. O'KEEFFE AND B. G. HYDE, *Struct. Bond.* **61,** 77 (1985).
18. R. D. BURBANK AND F. N. BENSEY, JR., U.S.A.E.C. Report K1280, United States Atomic Energy Commission, Washington, DC (1956).
19. A. C. LARSON, R. B. ROOF, JR., AND D. T. CROMER, *Acta Crystallogr.* **17,** 555 (1964).
20. R. PAPIERNIK, D. MERCURIO, AND B. FRIT, *Acta Crystallogr., Sect. B* **38,** 2347 (1982).
21. C. BROSSET, *Z. Anorg. Allg. Chem.* **239,** 301 (1938).
22. J. P. LAVAL, in preparation.